

# Particles held by springs in a linear shear flow exhibit oscillatory motion

Lukas Holzer and Walter Zimmermann\*

*Theoretische Physik, Universität Bayreuth, D-95440 Bayreuth, Germany*

(Dated: October 27, 2018)

The dynamics of small spheres, which are held by linear springs in a low Reynolds number shear flow at neighboring locations is investigated. The flow elongates the beads and the interplay of the shear gradient with the nonlinear behavior of the hydrodynamic interaction among the spheres causes in a large range of parameters a bifurcation to a surprising oscillatory bead motion. The parameter ranges, wherein this bifurcation is either super- or subcritical, are determined.

PACS numbers: 47.15.G-, 47.20.Ky, 47.57.J-, 47.61.-k

*Introduction.-* Studies about the motion of bacteria and flagella in a fluid, about the dynamics of blood cells and other small suspended objects such as polymers in simple flows are currently of central interest and count to one of the major issues of microfluidics [1, 2, 3, 4, 5, 6, 7, 8, 9, 10, 11, 12, 13]. According to the short spatial scales involved in these cases the fluid motion surrounding the particles can be described in the small Reynolds numbers limit [1, 2, 3, 4], by the linear Stokes equation [1].

The hydrodynamic interaction (**HI**) between neighboring blood cells, swimming bacteria, different segments of a polymer or between neighboring polymers is of nonlinear nature even in the limit of low Reynolds numbers [14]. Moreover, this nonlinear behavior may cause dynamical effects, such as the periodic motion of small sedimenting spheres [15, 16] or the synchronization effects between rotating strings and between cilia [17, 18], or it may cause a hydrodynamic coupling of particles in optical vortices [19]. The HI may also amplify thermal fluctuations of polymers [22] to mention only a few examples.

Free single polymers show already a complex dynamical behavior in shear flow [7, 8] and the hydrodynamic interaction between many polymers leads to the so-called elastic turbulence [5, 6]. Furthermore polymers fixed at one end in a plug flow are also a major issue [20, 21] where one finds in this case significant hydrodynamic interaction effects both for the static as well as dynamic properties of the tethered polymers [21, 22, 23]. Tethered polymers in shear flow have also been studied but so far only a single polymer fixed with one end at a wall was considered [24, 25, 26, 27]. Recently, investigations have been started in order to analyze the behavior of several flexible polymers fixed with their ends at the top of neighboring pillars [28] and exposed to a linear shear flow. So the interesting question arises quite naturally: what is the dynamics of neighboring tethered polymers in shear flow and which role plays the hydrodynamic interaction?

We mimic a situation of interacting tethered polymers by spheres anchored by springs and neglect in a first ap-

proach thermal fluctuations. To the best of our knowledge this is the first example where an oscillatory motion of bound particles in low Reynolds number flow has its origin in the hydrodynamic interaction.

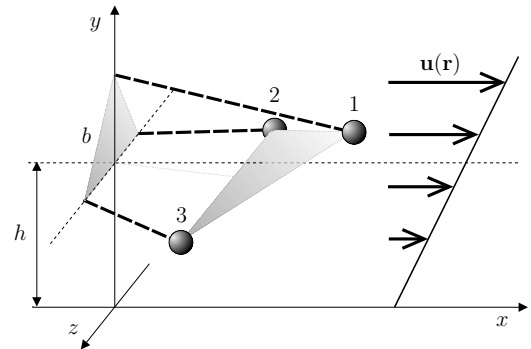


FIG. 1: The three particle configuration in shear flow is shown. The corners of the triangle in the  $y-z$ -plane mark the minima of the harmonic potentials of the beads. The flow induced sphere displacements are indicated by the dashed lines.  $h$  measures the shift of the lower side of the triangle from the center of the shear flow,  $\mathbf{u}(0) = 0$ .

*Model.-* Three beads are fixed in a shear flow by linear springs with a spring constant  $k$  as shown in Fig. 1. The locations of the minima of the corresponding harmonic potentials,  $\mathbf{R}_i$  ( $i = 1, 2, 3$ ), build, if not stated otherwise, an equilateral triangle of sidelength  $b$  and height  $H = b/\sqrt{2}$  with the upper corner at  $\mathbf{R}_1 = (0, h + H, 0)$  and the two lower corners at  $\mathbf{R}_{2,3} = (0, h, \pm b/2)$ . The bead-springs are elongated by a linear shear flow

$$\mathbf{u}_0(y) = (\dot{\gamma}y, 0, 0) \quad (1)$$

and the actual bead positions  $\mathbf{r}_i$  ( $i = 1, 2, 3$ ) are determined by the equations for the bead velocities

$$\dot{\mathbf{r}}_i = \mathbf{u}_0(\mathbf{r}_i) - \frac{k}{\zeta} \tilde{\mathbf{r}}_i + \sum_{j \neq i} (\mathbf{u}_\gamma(\mathbf{r}_{ij}) - \Omega^{RP}(\mathbf{r}_{ij}) k \tilde{\mathbf{r}}_j) \quad (2)$$

with  $\tilde{\mathbf{r}}_i = \mathbf{r}_i - \mathbf{R}_i$ . The first term describes the linear shear flow given by Eq. (1) and the second contribution is the ratio between the spring force and the Stokes friction  $\zeta = 6\pi\eta a$  that a single fixed particle of effective bead radius  $a$  experiences in a flow with shear viscosity  $\eta$ . Each

\*Electronic address: walter.zimmermann@uni-bayreuth.de

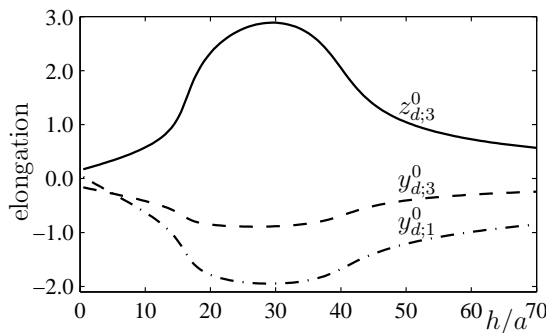


FIG. 2: The figure shows the stationary vertical displacements  $y_3^0 = y_2^0$  of the lower beads (dashed line) and  $y_1^0$  of the upper bead (dash-dotted line) as well as the shift  $z_3^0 = -z_2^0$  in  $z$ -direction (solid line) as a function of the vertical shift  $h/a$  and for the dimensionless shear rate  $\tau\dot{\gamma} = 2.6$ .

fixed particle causes a perturbation of the shear flow at the location of the other beads and vice versa. This so called hydrodynamic interaction (**HI**) is described for a Stokes flow by the Rotne Prager tensor [14]

$$\Omega^{RP}(\mathbf{r}) = \frac{1}{8\pi\eta r} \left( \left(1 + \frac{2a^2}{3r^2}\right) \mathbf{I} + \left(1 - 2\frac{a^2}{r^2}\right) \frac{\mathbf{r}\mathbf{r}}{r^2} \right), \quad (3)$$

which describes together with the harmonic forces  $k\tilde{\mathbf{r}}_j$  the fourth contribution in Eq. (2).  $\mathbf{I}_{ij} = \delta_{ij}$  is the unity matrix. The shear flow induces sphere rotations, which alter the flow field and therefore its action onto other spheres, as described by the third term in Eq. (2) [29]

$$\mathbf{u}_\dot{\gamma}(\mathbf{r}) = \left( -\frac{5}{2} \left(\frac{a}{r}\right)^3 + \frac{20}{3} \left(\frac{a}{r}\right)^5 \right) \frac{\mathbf{r} \cdot \mathbf{E} \cdot \mathbf{r}}{r^2} \mathbf{r} - \frac{8}{3} \left(\frac{a}{r}\right)^5 \mathbf{E} \cdot \mathbf{r}, \quad (4)$$

where  $\mathbf{E}_{ij} = \frac{\dot{\gamma}}{2}(\delta_{ix}\delta_{jy} + \delta_{iy}\delta_{jx})$  if the particle can rotate freely and  $\mathbf{E}_{ij} = \dot{\gamma}\delta_{iy}\delta_{jx}$  if an external torque prevents the rotation. With the relaxation time  $\tau = \zeta/k$  and the effective bead radius  $a$  one may rescale time  $t \rightarrow \tau t'$ , space  $\mathbf{r} \rightarrow a\mathbf{r}'$  and the shear rate  $\dot{\gamma}' \rightarrow \tau\dot{\gamma}$  and the results in this work are most conveniently presented in terms of these dimensionless units, as for instance the sphere displacement  $\mathbf{r}_{d;i} = \mathbf{r}'_i - \mathbf{R}'_i = (x_{d;i}, y_{d;i}, z_{d;i})$ .

*Stationary displacement of the spheres.*- The stationary solutions of the nonlinear equations (2), i.e.  $\dot{\mathbf{r}}_i = 0$ , with the displacements  $\mathbf{r}_{d;i}^0 := \mathbf{r}'_i^0 - \mathbf{R}'_i = (x_{d;i}^0, y_{d;i}^0, z_{d;i}^0)$  are determined numerically by a Newton algorithm.  $\mathbf{r}_{d;i}^0$  of a single bead increases according to the Stokes drag force  $\mathbf{F} = 6\pi\eta a\mathbf{u}$  and the linear spring force linearly with the flow velocity  $\mathbf{u}_0$ . However, by virtue of the nonlinear nature of the HI between the beads the elongation of the linear springs change nonlinearly as a function of the flow velocity, which itself varies linearly with the height  $h/a$ , as depicted in Fig. 2 for  $\tau\dot{\gamma} = 2.6$ .

For  $h = 0$  the flow velocity vanishes at the positions of bead 2 and 3 and with a finite shear gradient  $\dot{\gamma}$  only the upper bead 1 is displaced. The flow perturbation

caused by bead 1 shifts beads 2 and 3 slightly downward and pushes both away in  $z$ -direction with  $z_{d;3}^0 = -z_{d;2}^0$ . For finite  $h$  bead 2 and 3 are exposed to a finite velocity  $\mathbf{u}_0(\mathbf{r}_{2,3})$  and excite also flow perturbations pointing both downward at bead 1. This involves  $y_{d;1}^0$  to become negative as well and since both perturbations act downwards one has  $y_{d;1}^0 < y_{d;2}^0$  at intermediate values of  $h$ , cf. Fig. 2. In  $z$ -direction both disturbances compensate each other, so that  $z_{d;1}^0 = 0$  is left unchanged. According to this stronger displacement  $y_{d;1}^0$  at intermediate values of  $h$  the relative distance between the upper and the two lower beads is reduced and therefore the flow perturbations caused by bead 1 are enhanced, and so are the values of  $|y_{d;3}^0|$  and  $z_{d;3}^0 = -z_{d;2}^0$  as a function of  $h$ .

It is very surprising that all these displacements reach extrema, as shown in Fig. 2 and become smaller again for large values of  $h$ . An explanation of this behavior may be offered by inspecting the bead positions at large values of  $h/a$ . In this case the triangle built by the bead positions is again nearly parallel to the  $y-z$  plane and accordingly the flow perturbations and the related forces caused at the neighboring beads are nearly vanishing compared to their external force. In this limit, however, the height  $H$  of the triangle is smaller and the distance between the beads 2 and 3 is larger than for a vanishing fluid velocity. The latter behavior is a consequence of a complex balance between the spring forces and the nonlinear forces due to the flow disturbances. Correspondingly there is hitherto no simple qualitative picture for both, the deformed triangle built by the beads and the decreasing behavior of the elongation beyond their extrema.

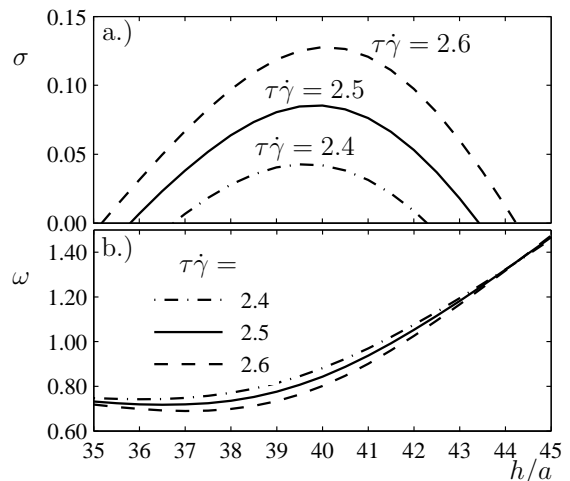


FIG. 3: The largest real part  $\sigma(h)$  is given in a) as a function of the vertical shift  $h/a$  for different shear rates  $\dot{\gamma}$  and part b) shows the corresponding imaginary parts  $\omega$ .

*Threshold of the Hopf bifurcation.*- Slightly beyond the extrema in Fig. 2 the stationary bead displacements become unstable and one finds by numerically integrating Eqs. (2) using a standard method a bifurcation to oscillatory bead motions. The threshold of this bifurcation may be determined by a linear stability analysis of the

stationary elongation  $\mathbf{r}_{d,i}^0$  with respect to small perturbations  $\delta\mathbf{r}_i(t)$ . Using the ansatz  $\mathbf{r}_i = \mathbf{r}_i^0 + \delta\mathbf{r}_i(t)$ , a linearization of Eqs. (2) leads to a set of 9 linear differential equations with constant coefficients

$$\dot{\mathbf{Y}} = \mathcal{L}(\mathbf{r}_i^0)\mathbf{Y} \quad \text{with} \quad \mathbf{Y}(t) = (\delta\mathbf{r}_1, \delta\mathbf{r}_2, \delta\mathbf{r}_3), \quad (5)$$

governing the linear dynamics of the perturbations  $\delta\mathbf{r}_i(t)$ . Eq. (5) is solved by  $\mathbf{Y} = \exp(\sigma t' \pm i\omega t')\mathbf{Y}_0$ , which transforms Eq. (5) into an eigenvalue problem. The eigenvalue with the largest real part  $\sigma(h)$  has also a finite imaginary part  $\omega$  and is positive within a finite range of  $h/a$  as shown in in Fig. 3 for three different values of the dimensionless shear rate  $\tau\dot{\gamma}$ . The whole range of a positive  $\sigma(h)$  in the  $\tau\dot{\gamma} - h/a$  plane is given by the shaded range in Fig. 4. The occurrence of oscillatory bead motion is

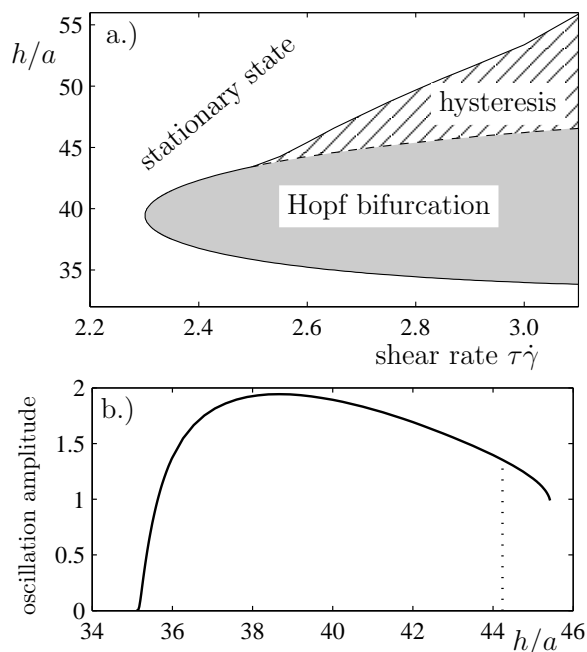


FIG. 4: a.) In the grey range the stationary bead elongation are unstable with respect to a supercritical Hopf bifurcation along the solid border line and to a subcritical one along the dashed line. Within the striped region the Hopf bifurcation is hysteretic. b.) The oscillation amplitude of bead 1 in  $x$ -direction is given as a function of  $h$  for  $\tau\dot{\gamma} = 2.6$ . The dotted line marks the upper threshold of the Hopf bifurcation.

rather robust with respect to changes of the anchor points of the linear springs which adhere the beads. We have tested this by changing the anchor point of bead 1 and 2 in all three spatial directions. With such modifications the three anchor points build either no equilateral triangle or the equilateral triangle is inclined and not anymore perpendicular to the flow direction. The major trends include the following ones. Bringing anchor points closer together enhances the hydrodynamic interaction which favors the Hopf bifurcation in a larger parameter range and it then takes also place at smaller shear rates and  $h$ .

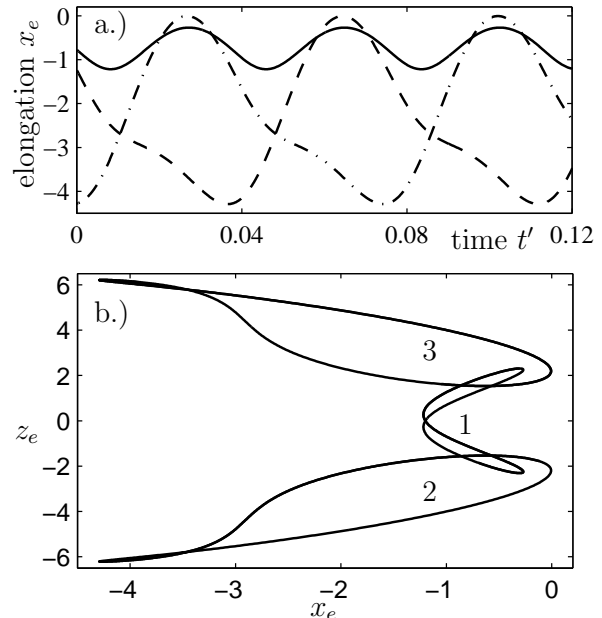


FIG. 5: a.) The time dependence of the deviation  $\mathbf{r}_{e,i}$  from the center of mass for bead 1 (solid line), 2 (dashed line) and 3 (dash-dotted line) for  $\tau\dot{\gamma} = 2.6$  and  $h/a = 35.5$ . b.) The corresponding bead oscillations in the  $x - z$  plane.

*Nonlinear behavior of the bead oscillations.*- A typical example for the three dimensional oscillatory motion of the beads is given by a projection onto the  $x$ -axis in Fig. 5a). Here the deviations  $\mathbf{r}_{e,i} = (x_{e,i}, y_{e,i}, z_{e,i})$  from the center of mass of the stationary solutions  $\mathbf{r}_{cm} = \sum_{i=1,2,3} \mathbf{r}_i^0/3$  are displayed. Two characteristic features can be recognized. Bead 2 and 3 oscillate with a phase shift of  $\pi$  and bead 1 oscillates along the  $x$ -direction with twice the frequency of the other two beads. The double frequency of bead 1 is an effect of the projection onto the  $x$ -axis, as can be seen from the phase portrait in Fig. 5b). Similar phase portraits can be obtained in the  $x - y$  and the  $y - z$  plane as well. Bead 1 performs a three dimensional motion and accordingly beads 2 and 3 are pushed away by a phase shift of  $\pi$  as indicated in Fig. 5a).

The Hopf bifurcation is supercritical along the solid line bounding the grey range in Fig. 4a). It is subcritical along the dashed one and the range of hysteresis is indicated by the striped range. The oscillation amplitude  $\delta\mathbf{r}_i^2$  of bead 1 is shown in Fig. 4b) as a function of  $h/a$  at the shear rate  $\tau\dot{\gamma} = 2.6$ . It indicates the supercritical behavior at the lower threshold and the hysteresis at the upper one. Close to the supercritical Hopf bifurcation the oscillations are harmonic. Further away from this threshold and in the parameter range with hysteresis in Fig. 4a) the periodic motion becomes rather anharmonic.

*Conclusions.*- We found in this work a Hopf bifurcation of three bounded spheres in a low Reynolds number linear shear flow, which is induced by the interplay of the nonlinear behavior of hydrodynamic interaction between the spheres and the shear gradient. To the best of our knowledge it is the first description of oscillations of bounded

and hydrodynamically interacting particles in a Stokes flow. Most of the results are obtained for three beads anchored by linear springs at the corner of an equilateral triangle which is perpendicularly oriented with respect to the flow direction. The phenomenon is very robust against various variations of the anchor points. For two beads we did not find oscillations.

Our results may also guide investigations on hydrodynamically interacting polymers fixed at small spheres and held by laser tweezers or anchored at boundaries in shear flow as well as for polymers that are fixed in shear flow close to boundaries at the top of pillars [28]. It is also an interesting question to be addressed, whether a recently discussed cyclic motion for grafted polymers [24, 26, 27] is related to the Hopf bifurcation discussed here.

We expect that several modifications of our model fa-

vor oscillatory motion too. For instance nonlinear spring constants (which may mimic tethered polymers), different spring constants in different directions or an exposition of the three beads to a Poiseuille flow with its spatially dependent shear rate. The effects of these and other extensions are the subject of forthcoming work.

### Acknowledgments

We are grateful to J. Bammert, R. Peter and F. Ziebert for useful discussions. We acknowledge financial support from the German science foundation (DFG) via the priority program SPP 1164.

- 
- [1] J. Happel and H. Brenner, *Low Reynolds Number Hydrodynamics* (Prentice-Hall, Englewood Cliffs, 1981).
  - [2] H. Berg, *Random motions in biology* (Princeton Univ. Press, Princeton, 1993).
  - [3] H. C. Berg and E. M. Purcell, *Biophys. J.* **20**, 193 (1977).
  - [4] P. Tabeling, *Introduction to Microfluidics* (Oxford Univ. Press, Oxford, 2006).
  - [5] A. Groisman and V. Steinberg, *Nature* **405**, 53 (2000).
  - [6] A. Groisman and V. Steinberg, *New Journal of Physics* **6**, 29 (2004).
  - [7] D. E. Smith, H. P. Babcock, and S. Chu, *Science* **283**, 1724 (1999).
  - [8] C. M. Schroeder, R. E. Teixeira, E. S. G. Shaqfeh, and S. Chu, *Phys. Rev. Lett.* **95**, 018301 (2005).
  - [9] N. Darnton, L. Turner, K. Breuer, and H. C. Berg, *Biophys. J.* **86**, 1863 (2004).
  - [10] H. Noguchi and G. Gompper, *Proc. Nat. Acad. Sci.* **102**, 14159 (2005).
  - [11] V. Kantsler and V. Steinberg, *Phys. Rev. Lett.* **95**, 258101 (2006).
  - [12] C. Misbah, *Phys. Rev. Lett.* **96**, 028104 (2006).
  - [13] M. B. Short *et al.*, *Proc. Nat. Acad. Sci. (USA)* **103**, in press (2006).
  - [14] J. Rotne and S. Prager, *J. Chem. Phys.*, **50**, 4831 (1969).
  - [15] L. M. Hocking, *J. Fluid Mech.* **20**, 129 (1964).
  - [16] R. E. Caflisch, C. Lim, J. H. C. Luke, and A. S. Sangani, *Phys. Fluids* **31**, 3175 (1988).
  - [17] M. Reichert and H. Stark, *Eur. Phys. J. E* **17**, 493 (2005).
  - [18] A. Vilfan and F. Jülicher, *Phys. Rev. Lett.* **96**, 058102 (2006).
  - [19] K. Ladavac and D. G. Grier, *Europhys. Lett.* **70**, 548 (2005).
  - [20] T. T. Perkins, D. E. Smith, R. Larson, and S. Chu, *Science* **268**, 83 (1995).
  - [21] R. G. Larson, T. T. Perkins, D. E. Smith, and S. Chu, *Phys. Rev. E* **55**, 1794 (1997).
  - [22] D. Kienle, R. Rzehak, and W. Zimmermann, *Nonlinear Stokes law and hydrodynamically enhanced fluctuations of polymers in flow*, unpublished, 2006.
  - [23] R. Rzehak, D. Kienle, T. Kawakatsu, and W. Zimmermann, *Europhys. Lett.* **46**, 821 (1999); R. Rzehak, W. Kromen, T. Kawakatsu, and W. Zimmermann, *Eur. Phys. J. E* **2**, 3 (2000); R. Rzehak and W. Zimmermann, *Europhys. Lett.* **59**, 779 (2002); R. Rzehak and W. Zimmermann, *Phys. Rev. E* **68**, 021804 (2003).
  - [24] P. S. Doyle, B. Ladoux, and J. L. Viovy, *Phys. Rev. Lett.* **84**, 4769 (2000).
  - [25] B. Ladoux and P. S. Doyle, *Europhys. Lett.* **52**, 511 (2000).
  - [26] Y. Gratton and G. W. Slater, *Eur. Phys. J. E* **17**, 455 (2005).
  - [27] R. Delgado-Buscalioni, *Phys. Rev. Lett.* **96**, 088303 (2006).
  - [28] Ch. Brücker, J. Spatz and W. Schröder, *Experiments in Fluids* **39**, 464 (2005).
  - [29] J. K. G. Dhont, *An introduction to dynamics of colloids* (Elsevier Science Ltd, 1996).